Semi-annual variation of the geomagnetic field

S. R. C. Malin[1], D. E. Winch[2], and A. M. Işıkara[1]

[1]*Boğaziçi University, Kandilli Observatory and Earthquake Research Institute, 81220, Çengelköy, Istanbul, Turkey*
[2]*School of Mathematics and Statistics, University of Sydney, F07, Sydney, NSW 2006, Australia*

Nighttime hourly mean values of D, H and Z (or X, Y and Z in a few cases) from 113 observatories for the interval 1964.0 to 1966.0 have been analyzed to determine the semi-annual variation. Results from the 84 observatories with dip latitudes between $\pm 60°$ have been subjected to spherical harmonic analysis to determine the coefficients of the internal and external parts. Only those coefficients that are found to be significantly different from zero at the 5 per cent level have been included.

One of the main objectives is to obtain a reliable estimate, with confidence limits, of the internal/external ratio at a very low frequency for constraining estimates of the deep conductivity of the mantle. It is shown that a model that includes only the principal P_1^0 term can lead to a seriously misleading internal/external ratio.

1. Introduction

The solar-cycle, the annual and semi-annual variations are the longest period peaks of external origin in the geomagnetic spectrum. Thus they are of particular importance for placing constraints on estimates of the lower-mantle conductivity. Global models have been made of the 11-year and annual variations (e.g. Malin and Işıkara, 1976; Harwood and Malin, 1977), but modelling of the semi-annual variation has hitherto been confined to the principal P_1^0 term (e.g. Banks, 1972). The particular importance of the semi-annual variation is that, apart from the 27-day recurrence tendency and its harmonics, it is the only significant spectral peak between the daily (24-hour) and annual lines (see Black, 1970).

It is important to distinguish between the semi-annual variation of the field itself, considered here, and the more widely studied semi-annual variation of magnetic activity (McIntosh, 1959; Gupta and Chapman, 1967; Russell and McPherron, 1973). The two phenomena both have extrema near the equinoxes suggesting a common origin. There are several possible mechanisms. Since we use data for quiet-Sun years and omit the 5 International Disturbed Days of each month, the contribution of magnetospheric compression is minimal. Also, by using only nighttime data, the effect of ionospheric currents is virtually eliminated. So the variation we are looking at here is likely to be due principally to semi-annual changes in strength or position of the ring-current. One possible mechanism is that more solar-wind ions are available for trapping when the Earth is at relatively high latitudes. The Earth is at high heliographic latitude ($>7.23°$) for the week centred on September 9 and is at low heliographic latitude ($< -7.23°$) for the week centred on March 7; both times precede the equinoxes by approximately two weeks. Another possibility is that the magnetosphere is more effective at trapping particles when it is symmetrical with respect to the Earth-Sun line, viz. at the equinoxes. The annual north-south migration of the ring-current postulated by Fukushima and Nagata (1968) and by Malin and Işıkara (1976) would cause it to pass directly over a low latitude observatory twice a year, resulting in a semi-annual variation. This effect has been investigated by McCreadie and Butcher (1993).

The purpose of the present study is threefold. Firstly, it presents the first detailed global model of semi-annual variation. Previous analyses have either been confined to a small number of observatories, with no attempt at global coverage, to investigate specific features (Campbell, 1980, 1981; Hibberd, 1985; Rangarajan and Bhargava, 1987; Butcher and Schlapp, 1992; Rastogi, 1993; Rastogi *et al.*, 1994), or have been concerned with only one, or a very few spherical harmonics (McLeod, 1994). Secondly, we provide data which, in combination with other investigations, should help to elucidate at least the ring current part of the mechanism for the semi-annual variation. Thirdly, it provides data at an important frequency for use in estimating the conductivity of the mantle.

2. The Data

The data are hourly mean values of the magnetic elements of declination, D, horizontal intensity, H, and vertical intensity, Z, (or, in a few cases, north intensity, X, east intensity Y, and Z) from magnetic observatories. They have been compiled and put into machine-readable form by D. E. Winch, with some corrections by U. Schmucker, and further corrections to Pilar and Teoloyucan. The data cover the interval from 1964.0 to 1966.0 for some 130 magnetic observatories.

For reasons given by Campbell (1980) and Malin and Winch (1966), and for compatibility with Malin and Işıkara (1976) we chose to analyse nighttime data, consisting of the mean of five hourly mean values centred on the hourly mean

Table 1. Fourier coefficients for semi-annual variation (nighttime data). Unit: 0.01 nT. Φ denotes dip-latitude.

Obs. Code	Co-lat. (°)	E. long. (°)	Φ (°)	X a_2	σ_a	b_2	σ_b	Y a_2	σ_a	b_2	σ_b	Z a_2	σ_a	b_2	σ_b
ALE*	7.5	297.5	82	552	79	−141	139	566	62	−564	54	802	102	−593	107
HIS*	9.4	58.0	79	−61	107	−139	95	−50	129	−931	78	630	257	−639	196
CCS*	12.3	104.3	84	−383	195	−220	149	−317	120	−323	81	161	238	−1475	322
THL*	12.5	290.8	82	−5	71	−190	128	−50	77	−445	96	52	50	−502	60
MBC*	13.8	240.6	85	−391	98	−195	91	−140	95	−128	113	−36	99	−946	77
RES*	15.3	265.1	88	−9	141	−419	176	−62	89	−310	88	103	69	−643	93
DIK*	16.4	80.6	78	−1040	145	1447	262	−212	186	−93	222	300	126	−1256	217
TIK*	18.4	129.0	76	76	175	1106	216	−174	90	−260	114	−513	186	−337	133
BRW*	18.7	203.2	71	−1062	512	1075	400	−644	333	−648	245	−715	388	−116	280
TRO*	20.3	19.0	66	−739	440	1303	479	182	94	−369	117	−181	286	−454	211
GDH*	20.8	306.5	73	−17	60	−224	84	−21	55	−364	91	−7	136	−460	165
MMK*	21.8	33.1	65	248	240	1138	225	−137	158	−393	147	−96	141	124	187
KIR*	22.2	20.4	66	−522	672	690	447	48	185	−202	174	−677	306	194	337
SOD*	22.6	26.6	65	−112	542	1047	310	−72	166	−255	81	−520	140	287	144
CWE*	23.8	190.2	62	47	116	324	150	185	51	−136	49	278	105	27	105
CMO*	25.1	212.2	65	12	202	166	162	87	117	−35	98	2	116	109	135
BLC*	25.7	264.0	82	−28	149	185	124	−27	152	−127	87	476	204	−636	194
LRV*	25.8	338.3	64	−513	514	1175	295	104	226	−588	141	−338	128	295	137
DOB	27.9	9.1	60	59	122	279	96	−40	78	−177	64	−21	187	463	170
NUR	29.5	24.6	58	21	48	101	61	−35	34	−34	63	−158	49	198	98
LER	29.9	358.8	58	6	36	207	97	19	44	−138	78	−20	157	381	132
LNN	30.0	30.7	58	12	36	114	48	−78	27	−97	62	−34	43	152	74
LOV	30.6	17.8	57	19	30	71	40	−35	75	−62	60	−94	49	175	47
FCC*	31.2	265.9	77	−431	221	588	179	−1509	203	−450	210	610	292	−1036	193
SIT*	32.9	224.7	60	72	70	164	138	81	52	−144	93	41	89	−54	124
SVD	33.3	61.1	58	−32	33	57	50	−11	51	−117	41	−51	22	−3	21
RSV	34.2	12.4	54	−37	37	142	51	−45	38	−83	69	−53	47	204	49
KZN	34.2	48.8	56	−56	33	151	49	2	32	−74	54	3	25	57	28
MOS	34.5	37.3	55	32	29	138	29	−48	40	−59	45	−45	13	44	17
ESK	34.7	356.8	53	−99	24	90	42	−25	37	−96	61	−44	47	105	51
MEA*	35.4	246.7	66	49	125	368	163	312	86	51	83	−159	143	140	168
MNK	35.9	26.5	53	87	37	−68	30	28	44	−76	26	−11	22	14	25
STO	36.2	357.5	52	−72	33	14	32	39	38	−124	28	11	28	70	25
WNG	36.2	9.1	51	30	18	−5	46	−2	41	−15	58	−77	26	98	29
WIT	37.2	6.7	51	−56	34	106	43	47	31	−34	60	−32	25	46	18
IRT	37.8	104.4	56	75	48	161	36	20	22	−80	21	−9	15	0	15
SWI	37.9	21.2	51	46	39	84	41	−4	39	−58	45	−396	34	123	24
NGK	37.9	12.7	50	1	35	40	23	−14	34	−51	69	−50	18	51	12
VAL	38.1	349.8	50	−45	34	165	38	37	32	−95	53	45	39	101	27
HAD	39.0	355.5	49	7	34	64	26	36	36	−93	37	−73	18	39	14
KIV	39.3	30.3	49	96	35	170	33	−83	23	−118	36	−6	11	189	16
DOU	39.9	4.6	48	24	34	59	37	−22	46	−105	41	−53	22	72	14
LVV	40.1	23.8	48	−34	32	52	42	−19	37	−75	33	38	21	−5	24
VIC	41.5	236.6	55	−132	42	75	72	34	42	−92	53	99	45	−40	60
WIK	41.7	16.3	46	30	36	106	35	−7	45	−66	52	−65	13	−14	12
FUR	41.8	11.3	46	44	22	65	32	5	42	−49	50	−38	15	14	10
CLF	42.0	2.3	46	157	73	77	25	−88	43	−78	59	−237	28	−269	22
HRB	42.1	18.2	46	−42	23	25	36	25	31	−32	40	31	12	−74	13
YSS	43.0	142.7	41	131	71	118	52	13	25	−73	19	−75	19	−183	24
THY	43.1	17.9	45	−60	64	153	30	−59	51	29	56	−161	26	85	27
MMB	46.1	144.2	38	30	47	84	61	22	18	−93	16	−53	14	−58	20
AGN*	46.2	280.7	60	−49	66	259	87	17	34	−50	37	−172	77	−341	64
VLA	46.3	132.2	40	59	59	77	33	242	25	−90	35	159	22	−161	21
PAG	47.5	24.2	40	27	51	121	17	−19	15	−18	39	−80	14	−86	10
AQU	47.6	13.3	39	5	42	143	37	−52	31	−53	30	−98	8	−101	20
LGR	47.6	357.5	39	−63	20	37	23	−12	31	−38	40	−66	17	7	21
TFS	47.9	44.7	41	30	47	149	35	10	32	−64	41	−120	10	−51	15

Table 1. (continued).

| Obs.	Co-	E.	Φ	X				Y				Z			
Code	lat.	long.		a_2	σ_a	b_2	σ_b	a_2	σ_a	b_2	σ_b	a_2	σ_a	b_2	σ_b
	(°)	(°)	(°)												
TKT	48.6	69.2	41	20	41	148	51	−81	39	−11	28	−33	18	−22	13
EBR	49.2	0.5	37	−645	95	91	45	18	55	−12	37	−183	20	541	25
COI	49.8	351.6	37	−34	29	159	41	−93	19	−122	30	13	19	−25	23
FRD	50.1	282.6	54	28	43	221	52	44	28	−38	29	−33	22	−54	15
TOL	50.1	356.0	36	−191	42	244	30	14	40	−97	19	−113	16	196	23
ASH	52.0	58.1	37	215	38	165	76	57	31	32	24	−191	15	−38	15
ALM	53.2	357.5	33	104	23	219	34	5	21	−24	30	−26	20	−43	18
KAK	53.8	140.2	30	99	60	118	47	35	17	−78	19	15	20	−54	20
TEH	54.3	51.4	34	−7	69	105	60	32	50	−45	39	−76	79	276	25
SSO	56.4	135.9	28	19	78	109	58	37	16	−77	14	−54	17	−48	30
DAL	57.0	263.2	44	47	47	217	41	62	31	4	25	−109	19	−269	11
TUC	57.8	249.2	40	−55	55	197	39	81	21	−2	26	−50	9	−57	13
KNY	58.6	130.9	26	89	50	107	41	−45	10	−64	12	−4	8	−37	14
MLT	60.5	30.9	25	91	58	176	47	82	19	40	17	−204	10	−107	8
HVN	67.0	277.8	36	174	92	249	100	−40	27	−186	25	−170	28	−5	21
HON	68.7	202.0	22	57	61	231	87	61	14	31	20	23	11	44	9
ABG	71.4	72.9	13	159	58	−18	49	105	16	−55	20	−234	33	−819	47
SJG	71.9	293.8	32	−113	41	330	48	264	14	−20	16	−71	14	−22	12
HYB	72.6	78.6	11	105	131	94	98	−22	58	106	89	130	52	−224	41
MBO	75.6	343.0	8	−51	51	289	52	5	18	57	20	−181	11	−219	10
GUA	76.4	144.9	6	48	27	154	74	−19	6	−26	12	−87	22	23	25
ANN	78.6	79.7	3	−161	87	−68	72	−346	36	286	71	−174	26	−96	31
AAE	81.0	38.8	−1	101	42	190	32	−151	33	−262	33	189	31	102	17
KOR	82.7	134.5	0	−351	225	−3	218	−59	25	−158	15	−472	108	−420	58
PAB	84.2	304.8	17	−4	46	352	40	98	17	−84	17	−141	10	−39	19
FUQ	84.5	286.3	18	120	72	93	45	−47	17	−47	13	−224	25	−199	40
BNG	85.6	18.6	−7	231	49	533	66	−21	14	−352	20	95	18	44	25
MFP	86.6	8.7	−8	85	54	163	42	−186	20	27	22	−34	11	−32	9
TTB	91.2	311.5	8	4	88	308	46	−32	30	−29	28	−76	31	−53	18
LWI	92.3	28.8	−16	−329	104	143	67	−36	19	37	20	−21	5	−64	9
PMG	99.4	147.2	−18	−44	33	190	41	30	17	−96	20	63	16	−120	16
HUA	102.0	284.7	1	68	62	491	39	59	19	21	15	5	15	−8	12
API	103.8	188.2	−16	−145	72	111	59	−155	21	−46	26	81	14	55	17
TAN	108.9	47.6	−35	18	43	222	52	−91	13	45	24	17	16	78	28
TSU	109.2	17.6	−38	−95	69	318	84	−39	27	−57	26	−11	24	81	23
PIL	121.7	296.1	−15	−458	64	125	65	−41	21	−30	19	−255	22	77	55
GNA	121.8	116.0	−48	31	37	96	61	−22	27	−66	21	13	14	−38	14
HER	124.4	19.2	−47	−14	51	179	68	−18	27	21	38	8	21	−18	28
TOO	127.5	145.5	−51	−10	48	77	38	39	40	−92	31	−19	21	46	24
AML	133.2	172.7	−51	257	68	150	55	187	48	−106	49	172	47	38	29
TRW	133.2	294.7	−22	49	99	−122	73	−64	55	−94	42	−248	90	−92	28
KGL	139.4	70.2	−50	−211	48	171	45	−86	46	167	45	51	26	−62	34
MCQ*	144.5	159.0	−68	−212	304	1027	185	207	160	244	100	120	137	−403	73
AIA	155.2	295.7	−38	30	37	189	35	2	30	56	32	110	26	−66	40
MIR*	156.6	93.0	−65	−125	157	364	76	59	116	−43	154	−18	123	1044	120
DRV*	156.7	140.0	−89	233	69	49	54	2	70	554	39	−689	178	1245	155
MAW	157.6	62.9	−53	−234	238	1113	247	−100	338	−1161	408	354	196	347	158
RBD	160.4	24.3	−47	107	249	457	140	−255	185	−376	110	354	268	−410	200
SNA	160.5	357.5	−45	−97	64	359	78	321	51	−210	59	430	90	−37	55
NVL	160.8	11.8	−46	127	138	791	97	548	101	346	72	76	61	−445	116
EGS	165.2	282.8	−49	76	105	123	103	131	86	−4	72	519	162	−84	216
HBA	165.5	333.4	−47	109	291	895	180	210	156	175	85	357	327	−584	151
SBA*	167.2	166.8	−74	−79	137	−246	137	112	42	162	35	−187	101	1284	117
VOS*	168.4	106.9	−68	1956	121	−668	157	−1707	102	895	145	−7	97	1025	130
BYR*	170.0	240.0	−61	−87	154	452	196	−20	385	589	497	−266	278	819	260
SPA*	180.0	0.0	−61	74	160	−80	124	971	152	−134	129	425	151	1820	151

*Not used in the spherical harmonic analysis.
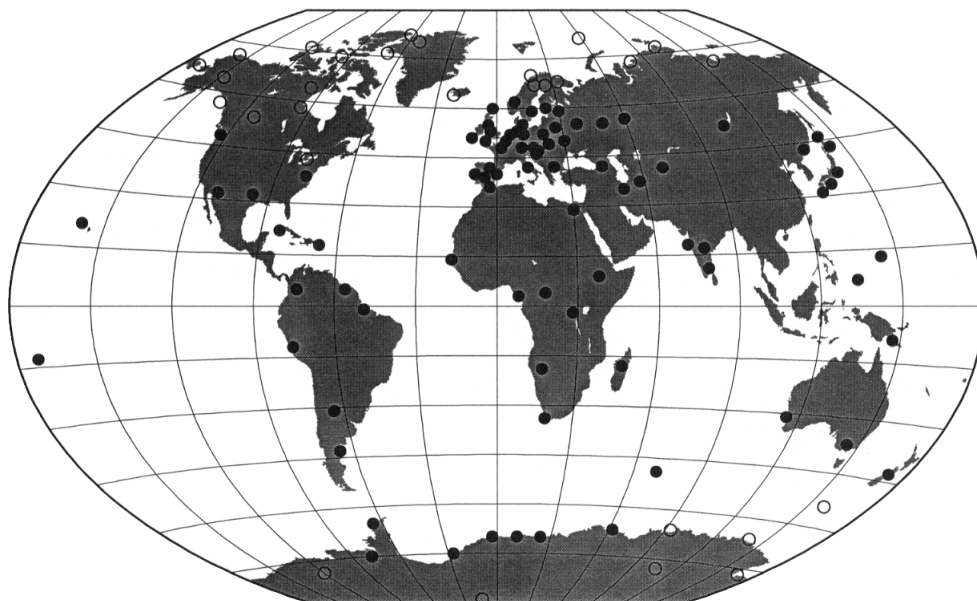
Fig. 1. Locations of the observatories listed in Table 1. Those marked by open circles are omitted from the spherical harmonic analysis.

value that includes local midnight, one mean for each day. These we call the "nighttime means".

3.   Method of Analysis

This is closely similar to that described by Malin and Schlapp (1980). For a given observatory, each nighttime mean provides an equation of condition of the form

$$H_{(t)} = H_0 + a_0 t + a_1 \cos t + b_1 \sin t + a_2 \cos 2t + b_2 \sin 2t,$$

where t increases from 0 to 2π from January 0.0 to December 31.0, H_0 represents a constant term, $a_0 t$ the secular variation (assumed to be linear over the 2-year interval analysed), $a_1 \cos t + b_1 \sin t$ the annual variation and $a_2 \cos 2t + b_2 \sin 2t$ the semi-annual variation.

The constants $H_0, a_0, a_1, b_1, a_2, b_2$, were determined, separately for each observatory and element, from the equations of condition by least-squares analysis of all the data. Their standard deviations were obtained as detailed by Malin *et al.* (1996). We denote those for a_2 and b_2 by σ_a and σ_b respectively. The values of a_2, b_2, σ_a and σ_b are the data for subsequent global analysis of the semi-annual variation.

All the H and D results were converted to X and Y.

4.   Quality Control

The nighttime means were plotted, together with curves synthesized from (H_0, a_0) and $(H_0, a_0, a_1, b_1, a_2, b_2)$. Each of these plots was examined for implausible values and for discontinuities, and these were checked against the original sources. Most of the apparently wild values were found to be real, but a few typographical errors (in the data for Pilar and Teoloyucan) were detected and corrected. The discontinuities resulted from unexplained changes of baseline. High quality baseline control is required for the reliable determination of the semi-annual term. Several of the observatories (particularly whose primary purpose was the monitoring of

shorter-period variations) either did not monitor their baselines, or had inadequate documentation of them. These observatories were rejected.

The results are given in Table 1, with the observatories listed in order of colatitude. Their geographic positions are shown in Fig. 1.

5.   Spherical Harmonic Analysis

We represent the global-scale features of the semi-annual variation with a spherical harmonic model of modest order and degree. Such a model would be expected to represent those parts of the variation that originate in the ring-current and magnetosphere, together with the induced reflection of these within the Earth. It could not hope to reproduce the high-latitude effects (ascribed by Malin and Işıkara (1976) to the auroral electrojets) where large fluctuations occur over a small range of latitude. Neither could it model any ocean-correlated effect, since the oceanic outlines require spherical harmonics of higher order and degree for their representation.

To avoid swamping the model with the large auroral-latitude variations, we followed the example of Malin and Işıkara (1976) in excluding from the analysis all observatories at high dip-latitude ($|\Phi| > 60°$, where $\tan \Phi = \frac{1}{2} \tan I_{\mathrm{m}} = Z_{\mathrm{m}}/2H_{\mathrm{m}}$; and I_{m}, Z_{m} and H_{m} denote the observatory values of dip, vertical and horizontal intensity, respectively, meaned over the data-interval). There were 29 such observatories. This left 84 observatories with X, Y and Z data suitable for spherical harmonic analysis, giving two sets of 252 equations of condition, one set for a_2 and one for b_2. The equations were weighted inversely as the variance of a_2 (or b_2) and solved by the method of least squares, using matrix inversion. The standard deviation of the spherical harmonic coefficients are given by $sd = (QW/N)^{1/2}$, where Q denotes the sum of squares of weighted residuals, W is the diagonal element of the inverse matrix corresponding to the required spherical harmonic and N denotes the number of degrees of freedom.

Table 2. Spherical harmonic coefficients of the semi-annual variation, including only harmonics with amplitudes significantly different from zero at the 95% level. The units are pT.

	Internal part		External part		
	a_2	b_2	a_2	b_2	*AIC*
Analysis for the optimum number of coefficients					
g_1^0	204 ± 95	-544 ± 111	-615 ± 178	-1836 ± 207	
g_1^1			-510 ± 86	-153 ± 106	
g_2^0			192 ± 87	542 ± 107	426.32
g_2^2	-137 ± 45	-108 ± 55	23 ± 53	244 ± 68	
g_3^3			27 ± 46	-297 ± 62	
g_4^1	-142 ± 45	-206 ± 49			
Analysis for the optimum number of coefficients, external and internal coefficients					
g_1^0	330 ± 112	-470 ± 131	-432 ± 208	-1832 ± 239	
g_1^1	86 ± 60	-99 ± 73	-385 ± 102	-182 ± 120	
g_2^0	-243 ± 87	-114 ± 107	-94 ± 123	376 ± 148	453.69
g_2^2	-162 ± 47	-83 ± 58	6 ± 57	250 ± 73	
g_3^3	-52 ± 41	24 ± 53	-1 ± 48	-280 ± 63	
g_4^1	-25 ± 57	-154 ± 64	169 ± 68	131 ± 76	
Analysis for the g_1^0 (dipole) term only					
g_1^0	273 ± 88	-533 ± 105	-333 ± 161	-1287 ± 191	451.48

Separate analyses are performed for a_2 and b_2, though both are part of the same harmonic. For this reason we choose to determine the same set of spherical harmonic coefficients for a_2 as for b_2. We judge the significance of a spherical harmonic term by R, the ratio of its amplitude to its vector standard deviation,

$$R = (A^2 + B^2)^{1/2}/(\sigma_A^2 + \sigma_B^2)^{1/2}.$$

Here, A and B denote corresponding spherical harmonic coefficients from the a_2 and b_2 analyses respectively, and σ_A and σ_B denote their standard deviations. If R exceeds 1.73 the harmonic is significantly different from zero at the 5 per cent level.

Which spherical harmonic coefficients should be included in the model? Tradition dictates that the model should be complete up to some chosen order and degree, but this is merely a hangover from the days of hand-computation and is no longer necessary. The larger the number of coefficients, the smaller will be the sum of squares of residuals and the closer the fit to the data. But closeness of fit is not a satisfactory criterion. When the number of coefficients equals the number of observations an exact, but not necessarily realistic, fit will be obtained.

Following Anderssen (1969), we consider the ideal model to be that that includes all the harmonics that are significant, and none that are not. Unfortunately, this does not define a unique model, since the significance of a coefficient depends on the set of other coefficients with which it is determined. We have found different, but self-consistent, sets of coefficients that satisfy the above criterion experimentally, and for different significance levels. In such cases, we opt for the model with the smaller standard deviations.

Our strategy to find a model that satisfies the requirements is as follows.

1. Choose a level of significance, e.g. $R > 1.73$ for the 95 per cent level, or $R > 1$ if we merely wish the harmonic to exceed its vector standard deviation (see Malin and Schlapp, 1980, Appendix).

2. Supply an initial set of harmonics. This can be the null set, but in our opinion it is preferable to do a few pilot analyses starting with a full set of harmonics and, for each successive analysis, dropping those that were not significantly determined. After a very few such iterations, all the remaining coefficients are significant, and this set of harmonics forms a suitable "initial set".

3. Up to a chosen upper limit, add the missing harmonics one at a time and re-analyse. If one of the added harmonics should yield a significant coefficient, it is included in the new "initial set" and the process starts again. Any harmonic that is insignificant in the presence of the new one is omitted.

When the process is complete, all the chosen coefficients
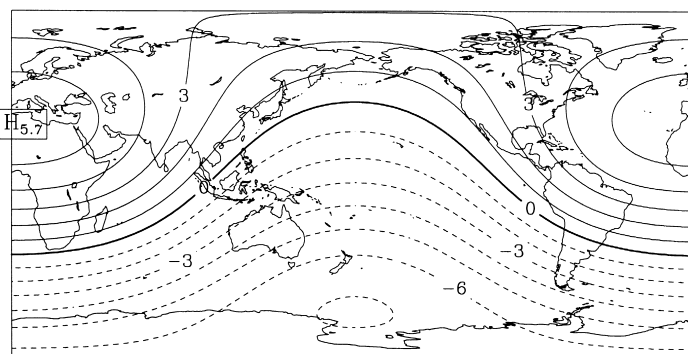
External current function 2 cpa A coeffs, kA
computed from midnight values
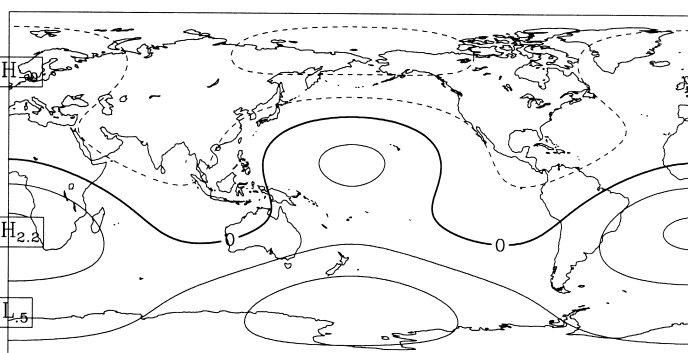
Internal current function 2 cpa A coeffs, kA
computed from midnight values

Fig. 2. The internal and external equivalent current systems for the semi-annual variation at January 0 (or July 2). Currents flow clockwise around positive contours, anticlockwise around negative; the units are kA. For April 1 (or October 1) the currents are reversed.

are significant, and no single one of those omitted would be significant if it were included with the final set.

We have arbitrarily chosen an upper limit of $m = n = 4$ for both the internal and external parts, giving a total of 48 available spherical harmonics. Here m denotes the order and n the degree of the spherical harmonic. It was not considered that the data were adequate in quality or distribution for the determination of higher order and degree coefficients.

6.   Results and Discussion

Table 2 gives the results of the analysis for the optimal model with only 6 spherical harmonics, there being 5 external and 3 internal coefficients for and for a_2 and for b_2. Also tabulated are the results when *all* 6 internal and external terms for a_2 and for b_2 are included, and given in the last row of Table 2 is the result for a model consisting of a dipole term only. Curiously, all the harmonics are g_n^m terms, being the coefficients of $P_n^m \cos m\lambda$ where λ denotes east longitude. None of the h_n^m terms (the coefficient of $P_n^m \sin m\lambda$) differs significantly from zero. The dominant harmonic is external g_1^0. The ratio of the internal to the external part of g_1^0 is 0.300 ± 0.064. This is unexpectedly large compared with 0.105 ± 0.032 found by Malin and Işıkara (1976) for

the annual term and 0.12 ± 0.07 for the 11-year variation (Harwood and Malin, 1977). It is closer to the ratio 0.37 found for the daily (24 hour) variation (Malin, 1973).

To show the significance of the chosen spherical harmonics in the potential for semi-annual variation, the Akaike Information Criterion (AIC), as defined by Akaike (1974) can be used, with N as the number of data points,

$$AIC = N \log(\text{mean square residual})$$
$$+2(\text{number of parameters}).$$

For the chosen model with 16 spherical harmonic coefficients, the sum of squares of residuals is 6541.73 and the *AIC* is 426.32. Other converged models, typically with 24 spherical harmonic coefficients, have a smaller sum of squares of residuals 6064.73, but a larger *AIC* of 452.78. The increased number of spherical harmonic coefficients gives a reduction in the sum of squares of residuals but an overall increase in the *AIC*. The model given in Table 1 has the smallest *AIC* of all converged models, as required for a preferred model.

The equivalent internal and external current functions associated with the model are shown in Figs. 2 and 3. Figure 2 shows the currents deduced from the analysis of a_2 which correspond to those flowing at the start and middle of the
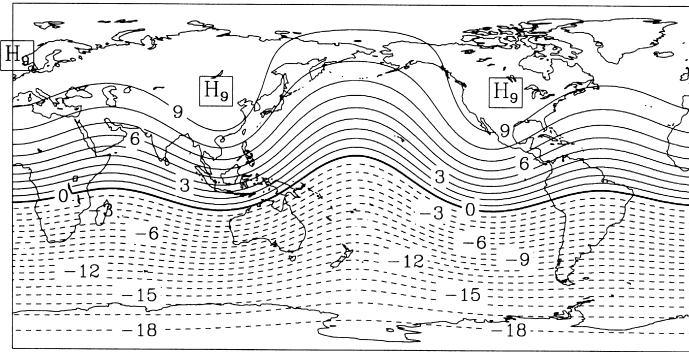
External current function 2 cpa B coeffs, kA
computed from midnight values
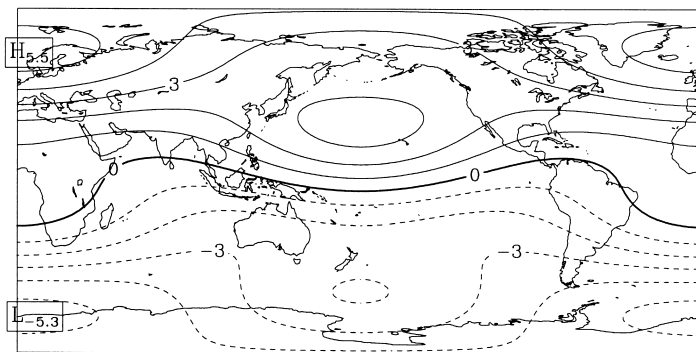
Internal current function 2 cpa B coeffs, kA
computed from midnight values

Fig. 3. The internal and external equivalent current systems for the semi-annual variation at February 15 (or August 16). Currents flow clockwise around positive contours, anticlockwise around negative; the units are kA. For May 17 (or November 16) the currents are reversed.

year. Figure 3, from the b_2 coefficients, represents the currents one eighth or five eighths through the year (February 15 or August 16). The currents are represented by flow parallel to the contours in a (hypothetical) thin spherical shell concentric with and of the same radius as the Earth. By far the largest currents are the external ones. The internal currents show interesting features over the Pacific Ocean, but this is probably because of the paucity of the data there, rather than a real effect. Note however, that the coefficients in the preferred model are all statistically significant at the 95% level, and every effort has been made to minimise the degree n of the analysis and the number of terms. The exclusion of high-latitude observatories has further reduced noise in the input.

Considering only the P_1^0 external coefficient, the maximum semi-annual variation is found to have a 95 per cent probability of occurring between January 30 and February 11. This is closer to the March 7 time predicted by the heliographic latitude hypothesis than to March 21 time of the equinoctial hypothesis, but is uncomfortably earlier than both predictions. For P_2^0, external, the extremum (this time a minimum) has a 95 per cent probability of occurring between February 21 and March 1, again favouring the heliographic

latitude hypothesis over the equinoctial.

It is common when determining g_1^0 for induction studies to do an analysis that includes no other terms. Since the observatories are far from being orthogonally distributed, the determined coefficients g_1^0 will contain a contribution from the undetermined harmonics. To see how serious this effect might be on the internal/external ratio we have done such an analysis. The results are given in the final row of Table 2. The greatest change is to the dominant term, for b_2 external, which is diminished by 30 per cent. The ratio of external to internal amplitude is 0.45 ± 0.10. Clearly, seriously misleading ratios can be obtained from such single term harmonic analyses, and this is likely to apply to frequencies other than the semi-annual.

References

Akaike, H., A new look at the statistical model identification, *IEEE Trans. Autom. Contr.*, **AC-19**, 716–723, 1974.
Anderssen, R. S., On the solutions of certain overdetermined systems of

linear equations that arise in geophysics, *J. Geophys. Res.*, **74**, 1045–1051, 1969.

Banks, R. J., The overall conductivity distribution of the earth, *J. Geomag. Geoelectr.*, **24**, 337–351, 1972.

Black, D. I., Lunar and solar magnetic variations at Abinger: their detection and estimation by spectral analysis via Fourier transformation, *Phil. Trans. R. Soc. London*, **A268**, 233–263, 1970.

Butcher, E. C. and D. M. Schlapp, The annual variation of the night-time values of the geomagnetic field, *Geophys. J. Int.*, **111**, 151–158, 1992.

Campbell, W. H., Secular, annual, and semi-annual changes in the base-line level of the Earth's magnetic field at North American locations, *J. Geophys. Res.*, **85**, 6557–6571, 1980.

Campbell, W. H., Annual and semiannual variations of the geomagnetic field at equatorial locations, *J. Atmos. Terr. Phys.*, **43**, 607–616, 1981.

Fukushima, N. and T. Nagata, Morphology of magnetic disturbance, *Ann. Geophys.*, **24**, 1–11, 1968.

Gupta, J. C. and S. Chapman, Some statistics concerning the daily geomagnetic character figure Cp, *Pure Appl. Geophys.*, **68**, 103–113, 1967,

Harwood, J. M. and S. R. C. Malin, Sunspot cycle influence on the geomagnetic field, *Geophys. J. R. Astr. Soc.*, **50**, 605–619, 1977.

Hibberd, F. M., The geomagnetic *Sq* variation—annual, semiannual and solar cycle variations and ring current effects, *J. Atmos. Terr. Phys.*, **47**, 341–352, 1985.

Malin, S. R. C., Worldwide distribution of geomagnetic tides, *Phil. Trans. R. Soc. London*, **A274**, 551–594, 1973.

Malin, S. R. C. and A. M. Işıkara, Annual variation of the geomagnetic field, *Geophys. J. R. Astr. Soc.*, **47**, 445–457, 1976.

Malin, S. R. C. and D. M. Schlapp, Geomagnetic lunar analysis by least squares, *Geophys. J. R. Astr. Soc.*, **60**, 409–418, 1980.

Malin, S. R. C. and D. E. Winch, Annual variation of the geomagnetic field, *Geophys. J. Int.*, **124**, 170–174, 1996.

Malin, S. R. C., M. K. Tunçer, and O. Yazici-Çakim, Systematic analysis of magnetic observatory data—1. A proposed method, *Geophys. J. Int.*, **126**, 635–644, 1996.

McCreadie, H. and E. C. Butcher, Preliminary analysis of annual and semi-annual variations of the geomagnetic field, *Explor. Geophys.*, **24**, 151–156, 1993.

McIntosh, D. H., On the annual variation of magnetic disturbance, *Phil. Trans. R. Soc. London*, **A251**, 525–552, 1959.

McLeod, M. G., Magnetospheric and ionospheric signals in magnetic observatory monthly means: electrical conductivity of the deep mantle, *J. Geophys. Res.*, **99**, 13577–13590, 1994.

Rangarajan, G. K. and B. N. Bhargava, Long term changes in the amplitude and phase of the semiannual and annual variations in low latgitude geomagnetic field, *J. Geomag. Geoelectr.*, **39**, 437–446, 1987.

Rastogi, R. G., Geomagnetic field variations at low latitudes and ionospheric electric fields, *J. Atmos. Terr. Phys.*, **55**, 1375–1381, 1993.

Rastogi, R. G., S. Alex, and A. Patil, Seasonal variations of geomagnetic *D*, *H* and *Z* fields at low latitudes, *J. Geomag. Geoelectr.*, **46**, 115–126, 1994.

Russell, C. T. and R. L. McPherron, Semi-annual variation of geomagnetic activity, *J. Geophys. Res.*, **78**, 92–108, 1973.

S. R. C. Malin (e-mail: malin@boun.edu.tr), D. E. Winch, and A. M. Işıkara